Separation and Purification Technology 300 (2022) 121826

Contents lists available at ScienceDirect

Separation and Purification Technology

journal homepage: www.elsevier.com/locate/seppur

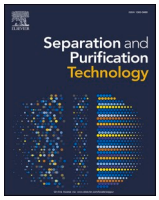

Graphene oxide nanosheets for drinking water purification by tandem adsorption and microfiltration

Sara Khaliha [a], Antonio Bianchi [a], Alessandro Kovtun [a], Francesca Tunioli [a], Alex Boschi [a], Massimo Zambianchi [a], Davide Paci [b], Letizia Bocchi [b], Sara Valsecchi [c], Stefano Polesello [c], Andrea Liscio [d], Michela Bergamini [e], Maurizia Brunetti [e], Maria Luisa Navacchia [a], Vincenzo Palermo [a,*], Manuela Melucci [a,*]

[a] Institute for Organic Synthesis and Photoreactivity (CNR-ISOF), Consiglio Nazionale delle Ricerche, via Piero Gobetti 101, 40129 Boloca (BO), Italy
[b] Medica Spa, via degli Artigiani 7, 41036 Medolla (MO), Italy
[c] Water Research Institute (CNR-IRSA), Consiglio Nazionale delle Ricerche, Via del Mulino 19, 20861 Brugherio (MB), Italy
[d] Consiglio Nazionale delle Ricerche - Istituto per la microelettronica e microsistemi (CNR-IMM), via del Fosso del Cavaliere 100, 00133 Roma (RM), Italy
[e] HERA SpA Direzione Acqua, Viale Carlo Berti Pichat 2/4, 40127 Bologna (BO), Italy

A B S T R A C T

Graphene nanosheets have outstanding adsorption efficiency toward organic molecules but the potential as sorbent for water purification is strongly limited by the tedious recovery of the nanosheets after the treatment, which can cause secondary contaminations. Here, we demonstrate that graphene oxide (GO) and reduced GO (rGO) nanosheets aggregation in tap water, enabling their separation by dead-end microfiltration (MF) on commercial polymeric hollow fiber modules. No evidence of GO/rGO contamination was found in microfiltered water and chemical potability of treated water was confirmed by standard protocols. Moreover, GO/rGO can be recovered (by inverting the filtration modality from IN-OUT to OUT-IN), washed and reused, this allowing the regeneration and reuse of both graphene nanosheets and the filtration module. The procedure (called here GO + MF) was optimized on tap water spiked with ofloxacin (OFLOX) or methylene blue (MB), as reference. The optimized procedure was then applied both with GO and rGO to the removal of a mixture of perfluoroalkyl substances (PFASs) from tap water at μg/L levels, the highest concentration found in water resources abstracted for water consumption. We demonstrate that rGO + MF procedure allows to remove 138 μg/g of total PFASs in only 30 min, i.e. an efficiency 3–5 times higher than granular activated carbon (43 μg/g) used in real potabilization plants for PFASs removal.

1. Introduction

The removal of emerging contaminants (ECs) is a research and industrial priority [1–4] requiring the urgent development of facile, sustainable, and highly efficient technologies in answer to the recently adopted European Drinking Water Directive 2020/2184 [5] and, more generally, to the UNs Sustainable Development Goal 6 'Ensure access to water and sanitation for all' [6].

Graphene oxide (GO) and reduced graphene oxide (rGO) nanosheets have shown outstanding adsorption properties toward several organic and metal ion water contaminants, with superior performances with respect to other carbon-based nanomaterials [7–16].

The outstanding performances of GO are due to the synergy between high surface area, multiple surface functional groups as interaction-binding promoting sites, and good water dispersibility [17,18]. Additionally, GO can be chemically manipulated in order to tailor its adsorption capability against pollutants [14,19–22]. GO nanosheets have shown adsorption maximum capacity of about 428 mg/g [17] for methylene blue (MB), a dye, 550 mg/g for rhodamine B (RhB), another dye, and 356 mg/g for ofloxacin (OFLOX), a fluoroquinolone antibiotic [23]. Metal ions such as Cu (II), Zn (II) and Pb (II) are effectively removed as well, with a maximum capacity of 117 mg/g, 345 mg/g and 1119 mg/g respectively [24]. Graphene oxide nanosheets have been also employed in combination with polymers like chitosan in the coagulation/flocculation process to remove turbidity and various contaminants [25].

Perfluoroalkyl substances (PFASs) [26] are a family of persistent compounds used in many industrial processes and everyday products, including polymers, pharmaceuticals, adhesives, insecticides and fire retardants, that have been found around the world in groundwater, surface water and even drinking water, and are a source of potentially severe health risk [27]. Several cases of contamination have been discovered around the world and Italy hosts the third most important case, in terms of extension of the polluted land: an area extending for

* Corresponding authors.
E-mail addresses: vincenzo.palermo@isof.cnr.it (V. Palermo), manuela.melucci@isof.cnr.it (M. Melucci).

https://doi.org/10.1016/j.seppur.2022.121826
Received 30 April 2022; Received in revised form 25 May 2022; Accepted 26 July 2022
Available online 29 July 2022

almost 200 km^2 between the counties of Padua, Verona and Vicenza (Veneto Region, Northern Italy). High concentrations of several PFASs have been observed in 2013 in freshwater and groundwater [28,29]. A significant social and scientific activity ended in the establishment of PFASs limits in drinking water in the recently adopted drinking water directive EU 2020/2184 [5].

Conventional purification technologies are partially ineffective in the removal of these substances from water and nanomaterials are expected to play a key role for enhanced purification from PFASs [30–34]. To date, only a few number of examples of treatment on PFASs by graphene materials has been reported [30,31,35,36], and most of them are limited to some specific molecules (e.g. perfluorooctanoic acid, PFOA, and perfluorooctanesulfonate, PFOS) [37–44].

Becanova et al. [36] recently described the fabrication of graphene and benzylamine modified graphene monoliths and their use as passive samplers for preconcentration of a mixture of PFASs in contaminante sites. Longer chain ($C \geq 8$) perfluoroalkyl acids (PFAAs) were adsorbed more efficiently than shorter chain PFAAs, which were better removed only upon modification of the monoliths with benzylamine moieties. In general, 3D graphene materials, such as foams and aerogels, are preferred as adsorbing materials for purification purpouses bacause of their ease of use and recovery, which can favour regeneration and reuse [11,45–49]. For some specific contaminants, i.e. methylene blue and heavy metals, their performance has been found to be competitive with granular activated carbon (GAC, the industrial standard), but their fabrication generally requires freeze-drying or other demanding processing that may limit future scale up.

Here, we demonstrate that commercial GO and rGO 2D-nanosheets can be used without any additional processing for adsorption of contaminants from water and then easily removed from the treated water by combining an innovative two steps method consisting of adsorption in batch and microfiltration (MF) on polyethersulfone hollow fiber (PES-HF) modules (Plasmart 100 module, Medica Spa). Such modules have a filtering surface of about 0.1 m^2, cut off of 1.000 KDa (inner diameter ≈280–300 μm, outer diameter ≈360–400 μm) and are a well-established technology for plasmapheresis (i.e. plasma purification) and drinking water disinfection, due to their removal of bacteria and microorganisms, with log retention LRV = 9 (i.e. 99,99999999 % retention) [50]. We demonstrate that PES-HF modules retain GO/rGO nanosheets quantitatively after the adsorption of microcontaminants from tap water. We studied GO and rGO (99 % reduced) having different surface chemistry and charge, to gain an insigth on adsorption mechanisms. The capacity of the procedure (from now on GO + MF) is demonstrated on OFLOX and MB, since they have strong affinity with GO but are not retained by PES-HF modules (neither by adsorption on PES polymer nor by physical filtration through the membrane porosity) [51]. Moreover, we demonstrate the suitability of this procedure for the removal of a mixture of fourteen selected PFASs in tap water at the maximum concentration so far found in contaminated sources.

2. Materials and methods

2.1. Materials

OFLOX and MB were purchased from Merck, Germany, and used without further purification. PFASs standard (CH_3CN:H_2O 9:1, 200 μg/mL) were purchased from Agilent Technologies (Santa Clara, CA, US). All the experiments on PFASs were carried out by using polypropylene vials. GO was purchased from Layer One (previously called Abalonyx) and used without further purification (graphene oxide powder < 35 mesh, product code 1.8, XPS: O/C ratio 0.39 ± 0.01, C 70.1 ± 0.9 %, O 27.2 ± 0.9 %, N 0.2 ± 0.1 %, S 1.0 ± 0.1 %, Si 0.8 ± 0.1 %, Cl 0.7 ± 0.1 %; manganese, a typical residue from synthesis, below 0.1 %) [52]. rGO was purchased from Layer One and used without further purification (rGO powder, fully reduced, carbon content of about 98.5–99 % weight). GAC was purchased from CABOT Norit Spa (Ravenna, Italy, Norit GAC 830 AF, MB index min 240 mg/g, BET surface area > 1000 m^2/g, see Fig. S1 and Table S1, SI for further details) [53]. In order to remove submillimetric particles (namely separating powder from granules), GAC was washed with deionized water at a mild flux, then dried overnight in an oven at 40 °C. River water was collected by the HERA Pontelagoscuro drinking water treatment plant after sedimentation, flocculation, filtration on sand and two stadium ozonization, but before GAC and final disinfection treatments.

Plasmart 100 MF module (Versatile® PES hollow fibers, membrane area filtering surface 0.1 m^2, pore average size 100–200 nm) were provided by Medica Spa (Medolla, Italy) [35].

2.2. Preparation of GO/rGO starting suspension and nanosheets morphology characterization

Typically, each batch of GO/rGO starting suspension consisted of a 2 mg/mL dispersion in deionized water (total volume 50 mL and total GO/rGO content 100 mg). The dispersion was sonicated for 4 h. The morphology of isolated GO deposited on silicon was studied by atomic force microscopy (AFM). Data were acquired in tapping mode employing a NTEGRA microscope of NT-MDT and rectangular silicon probes (RTESPA-300, Bruker, k = 40 N/m, ω = 300 kHz). Image processing and particle shape analysis was performed using SPIP software (Fig. S2, Table S2, SI). XPS spectra were acquired by hemispherical analyser (Phoibos 100, Specs, Germany), calibrated on Au 4f7/2 peak at 84.0 eV and using a Mg Kα excitation (Fig. S3, SI). AFM on rGO was not performed since rGO consists of larger aggregates rather than nanosheets. Aggregation experiments (Fig. S4, SI) were carried out starting from this suspension and diluting it in Milli-Q water, tap water and river water (Po river). Scanning electron microscopy (SEM) analysis were performed on GO and rGO both in Milli-Q water and tap water and SEM imaging were acquired with ZEISS LEO 1530 FEG (Fig. S5, SI). For the adsorption tests, the starting solution was diluted with tap water spiked with contaminants.

Size distribuition of GO/rGO aggregates in tap water was obtained by Laser Granuloumeter Saturn II (Micromeritics, Norcross, GA, USA). The quantitative study of lateral sizes was performed using percentile analysis [54].

2.3. GO/rGO loading capacity of MF modules

100 mL of GO/rGO starting suspension was filtered at 50 mL/min with a Cole-Parmer Masterflex® peristaltic pump on Plasmart 100 module in OUT-IN modality. This procedure was repeated with new batches of GO/rGO under the same conditions until saturation was reached (i.e. module clogging). The same protocol was applied also to determine the capacity of IN-OUT filtration modality.

2.4. Pores size and distribution of MF modules

The size of pores of PES-HF was obtained by using a liquid-liquid displacement porosimeter Poroliq1000 (Porometer, Germany-Belgium). The single fibre was sealed in loop shape with epoxy resin onto an inox stainless steel sample holder. Isobutanol-water was used as the wetting liquid, while water saturated with isobutanol was used as the displacement liquid. Through-pores size distribution was determined by using the Young – Laplace equation. A contact angle of 40° was measured for PES-HF with an OCA Dataphysics instrument.

2.5. GO/rGO release experiments

The presence of GO and rGO in filtered water after the tandem GO/rGO + MF experiments was checked by UV–Vis analysis in comparison to the spectra of standard suspensions at known concentrations (Fig. S6, SI) and total organic carbon (TOC) analysis in comparison to tap water (Table S3, SI). UV–Vis was performed by Cary 3500 UV–Vis

spectrophotometer (Agilent Technologies, Santa Clara, CA, USA).

2.6. Adsorption-microfiltration procedure optimization

In a typical experiment, GO starting suspension (total amount of GO 80 mg, total volume 40 mL) was added to a solution of OFLOX or MB in tap water (30 mg of OFLOX/MB in 60 mL, i.e. 0.5 mg/mL) and stirred for 30 min in darkness. The suspension obtained in this way was then filtered through a MF module, OUT-IN modality, at 55 mL/min using a Cole-Parmer Masterflex® peristaltic pump and the amount of OFLOX in filtered water was checked by liquid chromatography (HPLC-UV), according to an already reported protocol by using HPLC coupled with a variable wavelength detector (Agilent Technologies, 1260 Infinity; detection limit 25 ng/L) [51]. The maximum amount of OFLOX or MB removed by a single MF module was estimated by repeating the procedure with a new batch of GO + OFLOX/MB suspension until clogging of the module was reached (Fig. S7, S8 and S9, SI). Method optimization was made at different initial concentration of OFLOX (Fig. S10 and Table S4, SI).

2.7. Regeneration experiments

GO/rGO regeneration: GO starting suspension (total amount of GO 200 mg, volume 100 mL) was added to a solution of MB (300 mg/L, total volume = 250 mL) and stirred for 30 min as for the experiment described above in section 2.6. In the case of rGO basing on previously reported adsoprtion isotherms studies [17], a concentration of MB of 100 mg/L, and total volume of 250 mL were used. After this time, GO/rGO was centrifuged (18000 rpm, 5 min), washed with 200 mL of ethanol for three times, filtered on a fritted-disc Büchner funnel, dried under vacuum and reused for a second adsorption cycle. This process was subsequently repeated in order to perform a third and last cycle.

Module regeneration: GO/rGO starting suspension (total amount of GO 1.4 g, volume 700 mL, about 2 g/L) was added to an equal amount of tap water to induce flocculation and stirred for 30 min. The suspension was then filtered at 50 mL/min with a Cole-Parmer Masterflex peristaltic pump on a Plasmart 100 module in OUT-IN modality. GO was then extracted from the module through the application of alternated water (200 mL/min) and compressed air (4 bar) flows in IN-OUT modality and simple mechanical shaking of the module. In this way, 1.1 g of GO was collected (i.e. 75 % of the original amount). The recollected GO was then dispersed again in water and used for additional two cycles with an additional drop of GO maximum loading of about 35 %. Similarly, rGO was extracted by flowing water at 200 mL/min without the need of compressed air, in IN-OUT modality. In this way, 1.3 g of rGO were recollected (i.e. > 90 % of the original amount). The recollected rGO was used for additional cycles and recollected with yield higher than 90 % in each run.

2.8. Core-shell HF-GO module fabrication and use for comparative GO + MF and microfiltration experiments

The core shell PES-GO hollow fibers module was prepared by filtering 25 mL of the starting GO suspension through the module OUT-IN at 1 bar and then performing a thermal annealing at 80 °C for 12 h; [51] then the filtering-annealing cycle was repeated, giving the final device. Ultimately, 100 mg of GO were loaded and fixed on the outer wall of the fibers. Filtration experiments were performed in the same OUT-IN modality (tap water 100 mL, OFLOX 20 mg, contact time 30 min, flow rate 55 mL/min).

2.9. PFASs kinetic experiments

A standard solution of the fourteen PFASs in methanol was prepared starting from the commercial mixture (final concentration: 5 mg/L). GO powder (25 mg) was sonicated in 2.5 mL of distilled water for 2 h, then 22.5 mL of tap water were added (pH = 6.9). The suspension was spiked with 50 μL of the mixture of fourteen PFASs and the final concentration of each contaminant was 10 μg/L in a total volume of 25 mL. After a variable contact time (10 min, 30 min, 4 h and 24 h) on a rotary shaker, the samples were centrifuged 10 min at 10000 rpm and the amount of PFASs in filtered water was determined by UPLC-MS/MS (details in SI, section 7.1). The same procedure was applied to rGO (pH of the suspension was 7.2) and GAC (pH of the suspension was 7.3). In the case of GAC, no sonication was performed.

2.10. PFASs removal experiments

A standard solution of the fourteen PFASs in methanol was prepared starting from the commercial mixture (final concentration: 5 mg/L). GO or rGO (25 mg, Abalonyx, rGO 99 % reduced) were sonicated in 2.5 mL of distilled water for 2 h, then 22.5 mL of tap water were added (pH = 6.9). The suspension was spiked with 50 μL of the mixture of fourteen PFASs and the final concentration of each contaminant was 10 μg/L in a total volume of 25 mL. After 30 min of contact time on a rotary shaker the suspension was filtered in a OUT-IN modality at 55 mL/min using a Cole-Parmer Masterflex® peristaltic pump. The concentration of PFASs in filtered water was checked by UPLC-MS/MS (details in SI, section 7.1).

3. Results and discussion

3.1. GO/rGO aggregates size analysis and microfiltration demonstration

A GO suspension was prepared by dispersion of GO powder in deionized water and sonication for 4 h. Atomic force microscopy (AFM) analysis revealed a percentage of monolayers > 99.0 % with a median size (D50) of about 170 nm. Moreover, the 90 % of GO nanosheets (D90) have a lateral size lower than 600 nm (Fig. 1a, Fig. S2 and Table S2, SI). However, if the suspension was directly prepared in tap water under the same conditions, the dispersion was not stable and flocculation could be observed after a few minutes (Fig. 1b and Fig. S4, SI). Scanning electron microscopy (SEM) images of the GO suspension in tap water dropped on silicon substrate confirm the presence of aggregates, contrasting with the almost uniform distribution of single flakes of GO in Milli-Q water (Fig. S5, SI). The size of GO aggregates was analyzed by laser diffraction particle size analyzed (LG) since, given their intrinsic limits, AFM (size ≤ 100 μm) and dynamic light scattering (DLS, size ≤ 10 μm) attempts failed. The size distribution percentiles obtained was D10 = 8 μm, D50 = 41 μm and D90 = 64 μm (see also Table S2, SI). PES-HF mean pore size measured by porosimeter analysis (Fig. 1c, 1d and Fig. S2c, S2d, SI) was in the in the range of 200–250 nm with the minimum pore size close to 100 nm. Therefore, the size of aggregates was at least two orders of magnitude higher than the pore size of PES-HF, meaning that the sheets would be retained by microfiltration on MF modules in dead-end filtration modality, i.e. with flow passing through the membrane porous wall (OUT-IN modality, inset of Fig. 1c). Evidence of graphene aggregates within the pores of the membrane were observed by optical microscopy analysis (Fig. S8b, SI).

In the same conditions, a reduced GO (rGO) suspension was prepared and analyzed. As expected from the high reduction state of rGO, the suspension was less stable and faster precipitation of rGO was also observed in this case. The lateral size distribution was D10 = 6 μm, D50 = 16 μm and D90 = 32 μm (LG), slightly lower that GO, but of the same order of magnitude. GO and rGO have extremely different chemical structures, GO is highly oxidised, with O/C ratio of 0.4, with C-O functionalities representing almost 50 % of all carbon atoms. In contrast, rGO is a fully reduced material, where 99 % of atoms are carbon and only 1 % oxygen atoms, as revealed by XPS analysis (Fig. S3, SI).

Flocculation of GO/rGO in river matrix (details in materials and methods section) was also studied to unravel the potential of the proposed approach also for treating other water matrixes. As shown by

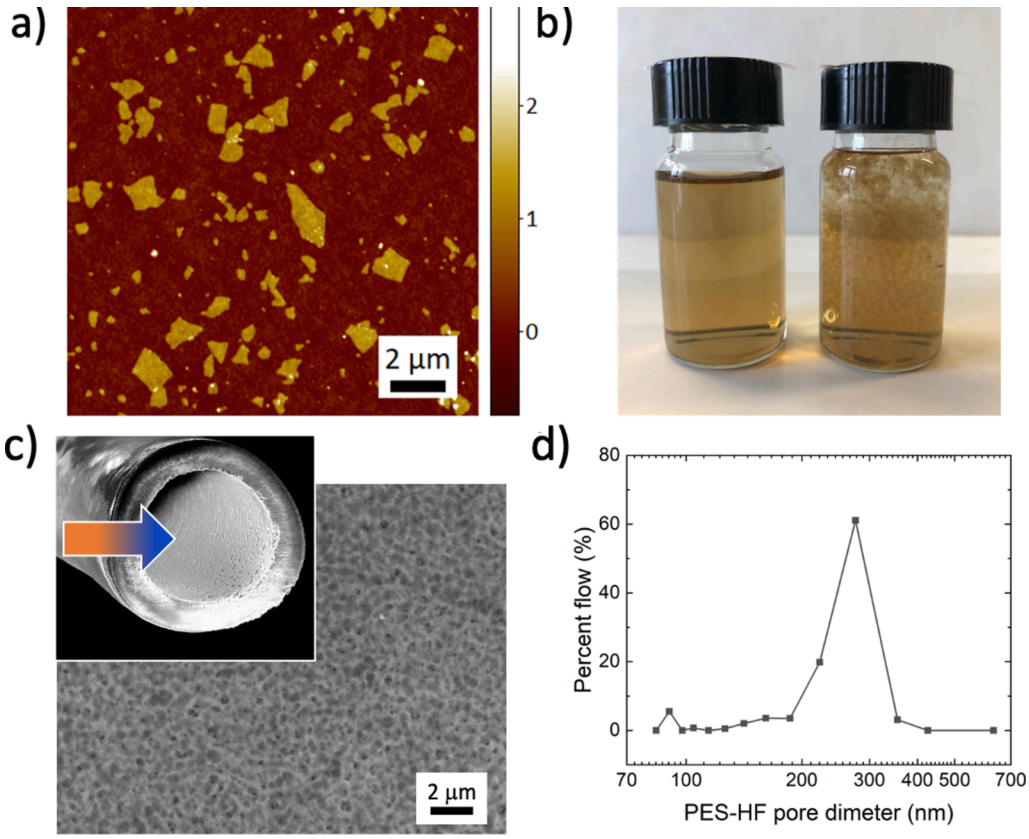

Fig. 1. Size analysis of graphene nanosheets-aggregates and of PES-HF pores. a) AFM image of GO nanosheets deposited from deionized water on silicon. b) GO dispersion in Milli-Q water (left) and tap water (right) after 30 min at concentration 0.1 mg/mL showing flocculation in tap water. c) Pores on the PES-HF fiber surface, the inset shows a PES-HF single fiber used for microfiltration and of the flow pathway in the OUT-IN modality. The fluid enters from the external wall of the hollow fibers and passes through the section to enter the fiber lume (lume diameter 300 µm. d) Pore size distribution measured with a liquid-liquid displacement porosimeter, from the pressure value of bubble point at 0.18–0.25 bar. Permability curve and repeated measurements are reported in Fig. S2c, S2d, SI.

Fig. S4, SI, flocculation was observed also in river water, with a much slower kinetic than that observed in tap water. Flocculation of GO in tap water has been already observed and ascribed to the effect of ions type and valence and to ionic strength that are almost negligible in deionized water [55,56]. River water has similar hardness (about 20 °F), but lower conductivity (432 vs 669 µS/cm a 20 °C, details in table S3, SI) and contains dispersed algae (210000 algae/L). The observed slower flocculation could be likely ascribed to the lower ionic strength of the river water matrix.

The exfoliated starting GO suspension in deionized water was then diluted with tap water to induce flocculation and then filtered until saturation of the MF module, highlighted by MF module clogging and drop of flow rate (from 50 mL/min to 15 mL/min), was reached. A maximum GO capacity of about 1.4 g was estimated for the MF module.

The opposite transmembrane filtration modality (IN-OUT), with the fluid entering the fiber lume and passing through the section to the external wall, was also considered. In this case, a maximum GO loading capacity of 800 mg was estimated, about half of the capacity of the OUT-IN modality. The higher value observed for the OUT-IN modality can be likely ascribed to the higher dead volume of the outer inner-fiber space. OUT-IN modality was selected as the ideal configuration and used for the following water purification experiments. Almost similar behaviour was observed for rGO with higher loading (about 1.7 g) in the OUT-IN modality. Optical microscopy analysis of the fibers after GO/rGO loading showed the presence of aggregates retained into fiber section pores (Fig. S8b, SI).

Fig. 2 shows the comparison between high speed centrifugation and microfiltration procedures on GO and rGO. Incresing centrifugation time up to 30 min at the maximum speed did not affect the precipitation yield. It can be clearly seen that centrifugation leads to uncomplete precipitation, in particular in the case of rGO. As a result, reiterated centrifugations are required, while in the case of MF treatament a clear solution is oberved after a single step. It should be pointed out that beside the highest operational simplicity of MF, the MF cartridges have standard cut-off, this ensuring that protocol reproducibility is independent from the operators, treatment time and scale.

Standard chemical potability of treated water in accordance to current EU regulation (D. Lgs. 31/01) was confirmed for treated water (Table S3, SI) [56]. The analysis also confirmed the absence of secondary contamination by metal ions that could be released from GO nanosheets (i.e. manganese-containing chemicals are used during GO synthesis). Moreover, in order to check the presence of possible release of GO from the module, we performed UV–Vis analysis on treated water (after concentration by rotary evaporation) and compared the spectra to those of GO suspensions at concentrations in the range of 2.5–10 mg/L (Fig. S6a and S6c, SI). After filtration, the sample was clear and no traces of GO in filtered water, within the LOD of the method (~2.5 mg/L), were found in the UV–Vis spectrum. This finding was in good agreement with the total organic carbon (TOC, Table S3, SI) measurements, being 3 mg/L for GO + MF solution and 2 mg/L for pristine tap water. rGO retention was tested as well, comparing the UV–vis analysis of a suspension of rGO 1 mg/mL, before and after filtration on MF module, with a standard solution of rGO 5 mg/L and no evidence of rGO was found in treated water (Fig. S6b, SI).

Notably, GO/rGO could be recovered after use, allowing regeneration and reuse (see also section 3.3). Inversion of water flow direction through the MF cartridge, enable GO/rGO aggregates detaching from the HF surface and pores cavities. A volume of water from 0.2 to 0.35 L per gram of rGO/GO was required to yield a recovery of about 80 %.

3.2. *Optimization of the adsorption-microfiltration procedure (GO + MF)*

After establishing the capability of MF modules to retain GO nanosheets, adsorption experiments were performed for the removal of OFLOX and MB in spiked tap water by exploiting the experimental setup shown in Fig. 3. OFLOX was selected as a reference substance due to its

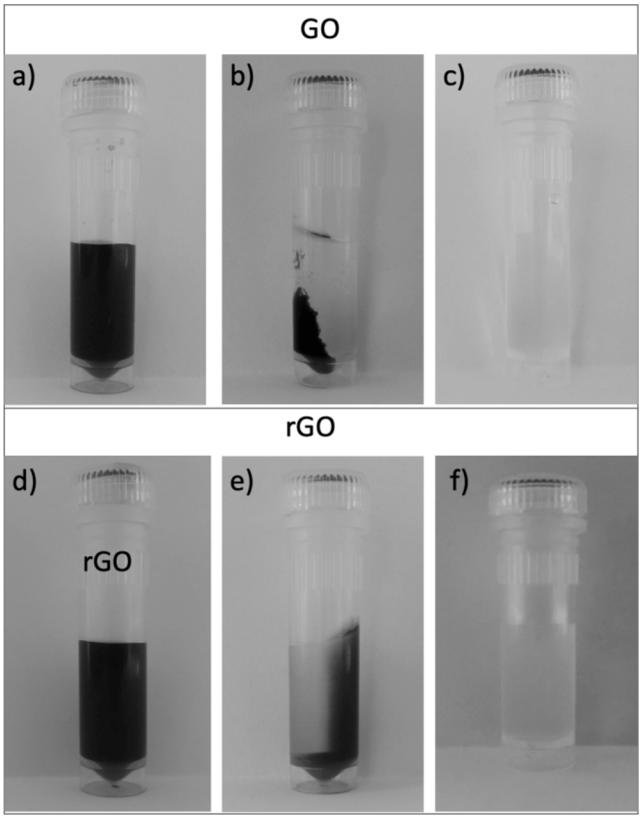

Fig. 2. Centrifugation of GO/rGO vs MF treatment. A suspension of GO or rGO in deionized water was diluted with tap water, as for water treatment experiments, then centrifugated at 10000 rpm for 10 min or microfiltered. Top: GO suspension before centrifugation (a), after centrifugation (b), and after MF (c). Bottom: rGO suspension before centrifugation (d), after centrifugation (e), and after MF (f).

strong affinity for GO (maximum adsorption capacity of GO nanosheets > 300 mg/g of GO) [23,57], quick equilibrium time [58–60], and ease of detection. MB was selected because it is considered the standard for adsorption tests on carbon materials (Fig. S7, SI).

Firstly, we excluded any possible contribution of PES-HF to the adsorption of OFLOX [51] and MB (Fig. S9, SI). Then we performed removal exeriments on OFLOX and MB. We found that the removal of OFLOX at initial concentration in the range 25–300 mg/L, was independent on the initial concentration, with values ranging between 99.8 % and 86.8 % (Fig. S10 and Table S4, SI). In order to facilitate the analytical detection, we performed all the subsequent experiments at an initial concentration of 300 mg/L. In a typical experiment, a sample of tap water spiked with OFLOX or MB was added to the starting GO suspension, stirred for 30 min in darkness, then filtered through a MF module and the amount of OFLOX or MB in filtered water quantified by HPLC (OFLOX) or UV–Vis (MB) analyses.

The maximum amount of OFLOX removed by a single MF module was then estimated by repeating the GO + MF experiments on the same MF module until clogging was reached, filtering at each repetition a new aliquote of GO and OFLOX solution (300 mg/L). In these conditions, we were able to remove about 240 mg of OFLOX per gram of GO (60 % of removal each repetition) and 356 mg for MB per gram of GO by using a single MF module (Fig. 4). It should be noted that the maximum adsorption capacity estimated at the equilibrium by adsorption isotherms of granular activated carbon (GAC), the industrial benchmark for adsorption on OFLOX and MB, are 95 mg/g and 187 mg/g respectively [17], and that <5 % of removal was observed for GAC after 30 min treatment.

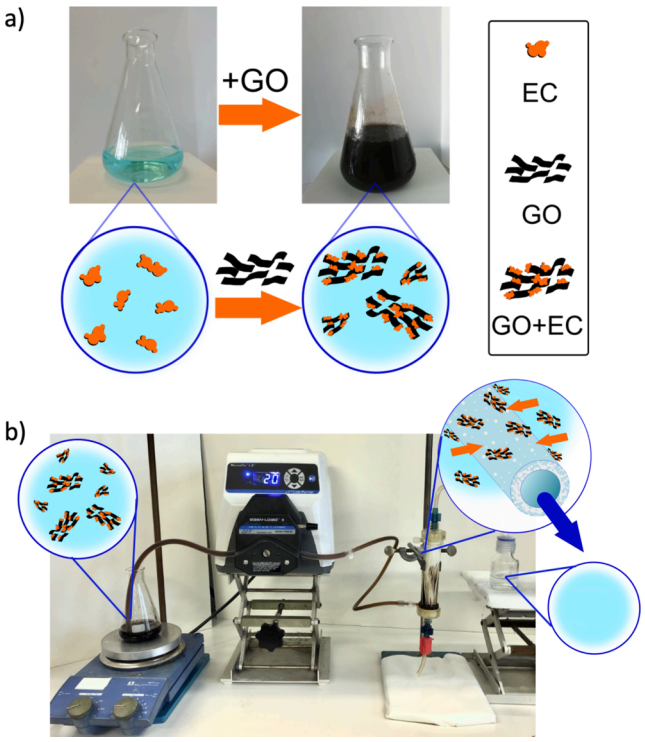

Fig. 3. Sketch of the adsorption-microfiltration process (GO + MF) for ECs removal. a) Adsorption: GO nanosheets are introduced in tap water spiked with OFLOX or MB and the solution is stirred at room temperature for 30 min in darkness; b) filtration: the suspension is filtered through the MF module in OUT-IN transmembrane modality.

3.3. Regeneration of exhausted GO/rGO nanosheets

After recovering of exhausted GO/rGO materials as previously described in section 3.1, regeneration possibility was also investigated and the whole procedure is schematized in Fig. 5. To this aim, after adsorption of MB, recollected sheets were washed with ethanol (about 10 mL of ethanol per mg of MB), recovered by centrifugation and final filtration, dried and reused in a second run of adsorption. In the case of GO, a drop of removal from 99 % → 90 % → 70 % was observed on going from the first to the third run, likely due to loss of material during each washing/filtration phases. Neverthless, it should be pointed out that in this experiment a very high concentration of MB was used in order to saturate GO (i.e. 75 mg MB in 250 mL of water, 300 mg/L). Similar trend was observed for rGO.

3.4. Two step GO + MF vs one step PES-GO core shell HF performances

The performance of the procedure GO + MF was finally compared to that obtained by using a core-shell PES-GO hollow fibers (HF-GO) module, having a multilayer GO coating fixed to the PES fiber wall. We recently demonstrated that adsorption of organic contaminants in core-shell HF-GO modules occurs by intercalation of the molecules in between overlapped GO layers [51]. The core-shell HF-GO module was created by fixing 100 mg of GO on the outer wall of the fibers (details in section 2.8) and the comparative experiments were performed at an OFLOX initial concentration of 200 mg/L (see Table S4, SI). Fig. 6a and 6b depict the two different processes: i) GO nanosheets adsorb OFLOX and the OFLOX loaded GO sheets are then filtered by the MF module in OUT-IN modality (Fig. 6a), ii) OFLOX spiked water is filtered by a core-shell HF-GO module having the same overall amount of GO pre-immobilized on the fiber surface outer wall in OUT-IN modality (i.e. the flow is forced to pass the GO multilayer, Fig. 6b). In the first case, the adsorption process mainly relies on the interactions of OFLOX molecules

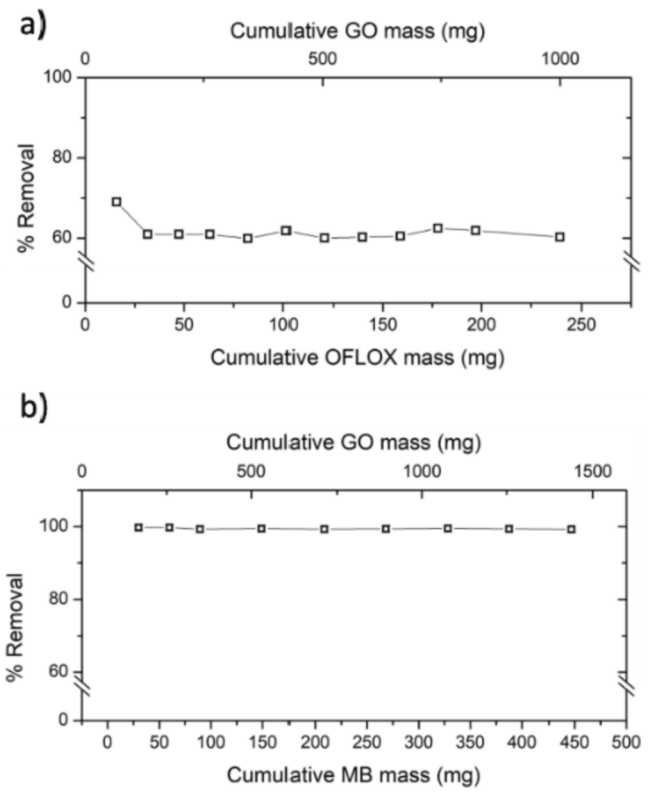

Fig. 4. Performance of the GO + MF procedure on OFLOX and MB removal. Estimation of maximum mass removal for a) OFLOX and b) MB. Each adsorption experiment was performed on the same MF module until clogging was reached (Fig. S7 and S8, SI). Experimental conditions for each repetition were: OFLOX/MB 30 mg, GO 80 mg; contact time 30 min; flow rate 55 mL/min; treated volume 100 mL.

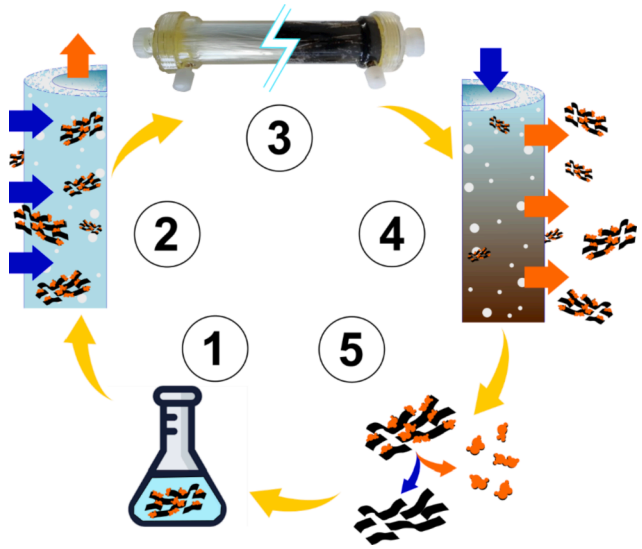

Fig. 5. Regeneration scheme of exhausted GO/rGO and saturated filter. 1) GO/rGO is added to polluted water and stirred for 30 min in order to perform the adsorption, 2) exhausted GO/rGO is filtered in OUT-IN modality through a MF module, 3) this two-steps procedure is repeated until the clogging of the module occurs, 4) GO/rGO is recollected from the filter through the use of water and compressed air fluxes in IN-OUT modality, 5) contaminants are extracted from GO/rGO by washing with ethanol three times, thus regenerating the adsorbing material. Regenerated GO/rGO and MF module are then ready for further adsorption cycles.

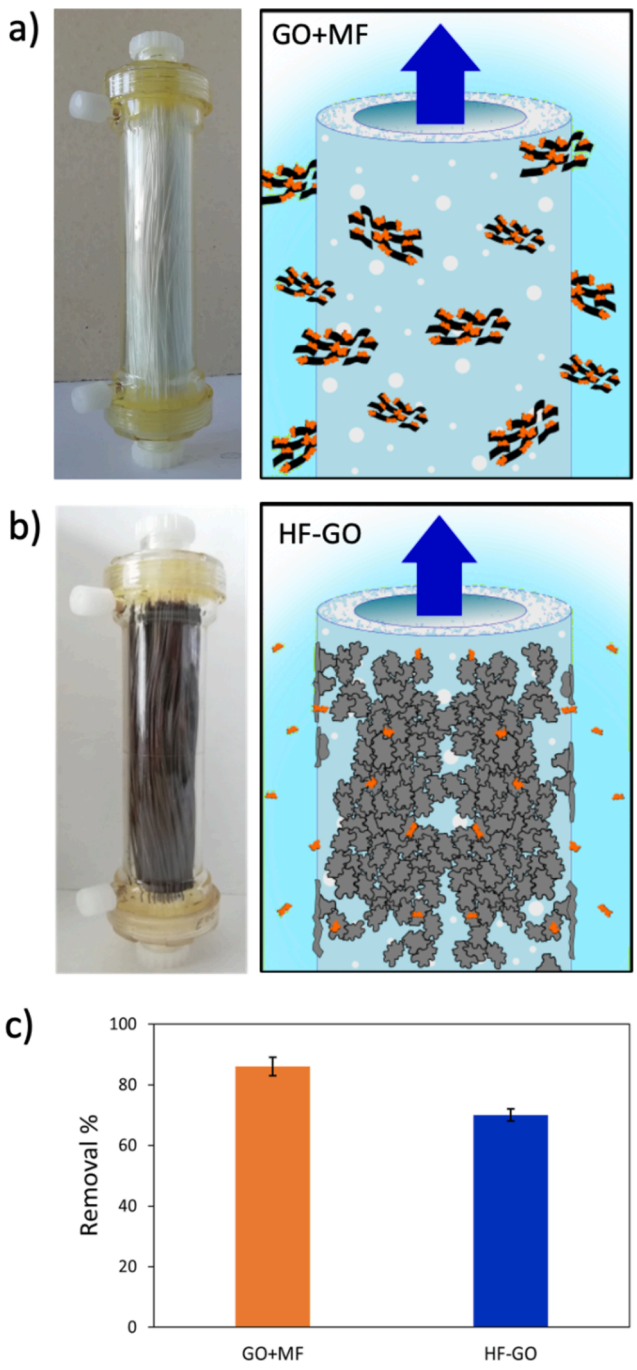

Fig. 6. Comparison between GO + MF procedure here proposed and MF on GO coated HF fibers. a) MF module used for the adsorption-microfiltration process and sketch of the working mechanism. b) Core-shell HF-GO module (left) and sketch of the working mechanism (right, details in section 2.8). Intercalation of OFLOX between the overlapped GO sheets in the multilayer has been already demonstrated [51]. c) Comparison between purification performances of adsorption performed by monolayer GO followed by microfiltration (GO + MF; orange bar) and simultaneous adsorption-microfiltration performed by GO multilayer (HF-GO; blue bar). Experiments repeated twice on two different modules.

with the functional groups on GO nanosheets, including π–π interactions, H bonds and hydrophobic interactions. In the latter case, adsorption occurs through the interplay of surface interactions and intercalation [51].

The removal efficiency estimated by UV–Vis analysis for the GO + MF procedure was 86 % (174 mg/g), and 70 % (140 mg/g) for the core-

shell HF-GO module (Fig. 6c), meaning that intercalation of molecules in GO multilayers overcomes the loss of surface area of the monolayer nanosheets. However, while the GO + MF procedure can be reiterated many times with almost the same performance (Fig. 4a) until saturation of the MF module by GO and allow regeneration of both GO and MF cartidge and reuse for three consecutive cyles, the core-shell HF-GO module performance drops from 70 % to 21 % after the second step.

3.5. Application of GO/rGO + MF to PFASs removal from tap water

The optimized procedure was then exploited for the removal of a mixture of PFASs of different alkyl chain length ($3 \leq CF_2 \leq 13$) from spiked water at the maximum concentrations (10 μg/L) detected in contaminated groundwaters in Veneto Region (Italy) [28]. GO and rGO performances vs GAC are summarized in Fig. 7a and 7b.

Adsorption-only tests on GO nanosheets (Fig. 7a, grey bars) showed increasing removal on increasing alkyl chain length for molecules ending with a carboxylic group, i.e. perfluorobutanoic acid (PFBA, 3 CF_2, <5 %), perfluorononanoic (PFNA, 8 CF_2, <20 %), perfluorotridecanoic acid (PFTrDA, 12 CF_2, >99 %). Higher performances were observed for sulfonated compounds rather than for carboxylic analougues, and on the increase of chain length, i.e. perfluorobutanesulfonic acid (PFBS, 4 CF_2 < 5 %), perfluorooctanesulfonic acid (PFOS, 8 CF_2 = 43 %). After the MF step (Fig. 7a, yellow bar), removal was significantly higher for all compounds (PFBS increased from < 5 % to 91 %) thanks to the contribution of the PES-HF to the adsorption. It can also be seen that rGO was more effective than GO (Fig. 7b; orange bars) in PFASs removal with increasing performance on increasing PFASs chain length, i.e. 21 % for PFBA (3 CF_2), 61 % perfluoropentanoic acid (PFPeA, 4 CF_2), 95 % perfluorohexanoic acid (PFHxA, 5 CF_2). Sulfonated compounds are better removed than carboxylic molecules, i.e. 96 % PFBS (4 CF_2) vs 61 % PFPeA (4 CF_2). No significant contribution of the MF step on the removal efficiency was observed, as shown by the comparison with the experiment including the MF step (Fig. 7b, blue bars) and with rGO adsorption alone (Fig. 7b, orange bars).

The lower performance of GO with respect to rGO on both short chain and long chain sulfonated and carboxylic compounds could be likely ascribed to the different surface charge of GO and rGO. Indeed, the Z potential of GO was −43.5 mV (tap water, after 2 h sonication) while that of rGO was −35.3 mV. The more negative surface charge of GO leads to a higher repulsive electrostatic interactions with PFASs molecules, which are mostly present in solution as dissociated anions at neutral pH (such as in our experimental conditions) [61,62]. On the other hand, the enhancement of performance on increasing the perfluoralkyl chain length can be related to the higher hydrophobicity of the PFASs molecules with octanol-water partition coefficient (log Kow) values in the range 2.3–8.9 (PFBA, 3 CF_2, and PFTeA, 13 CF_2,

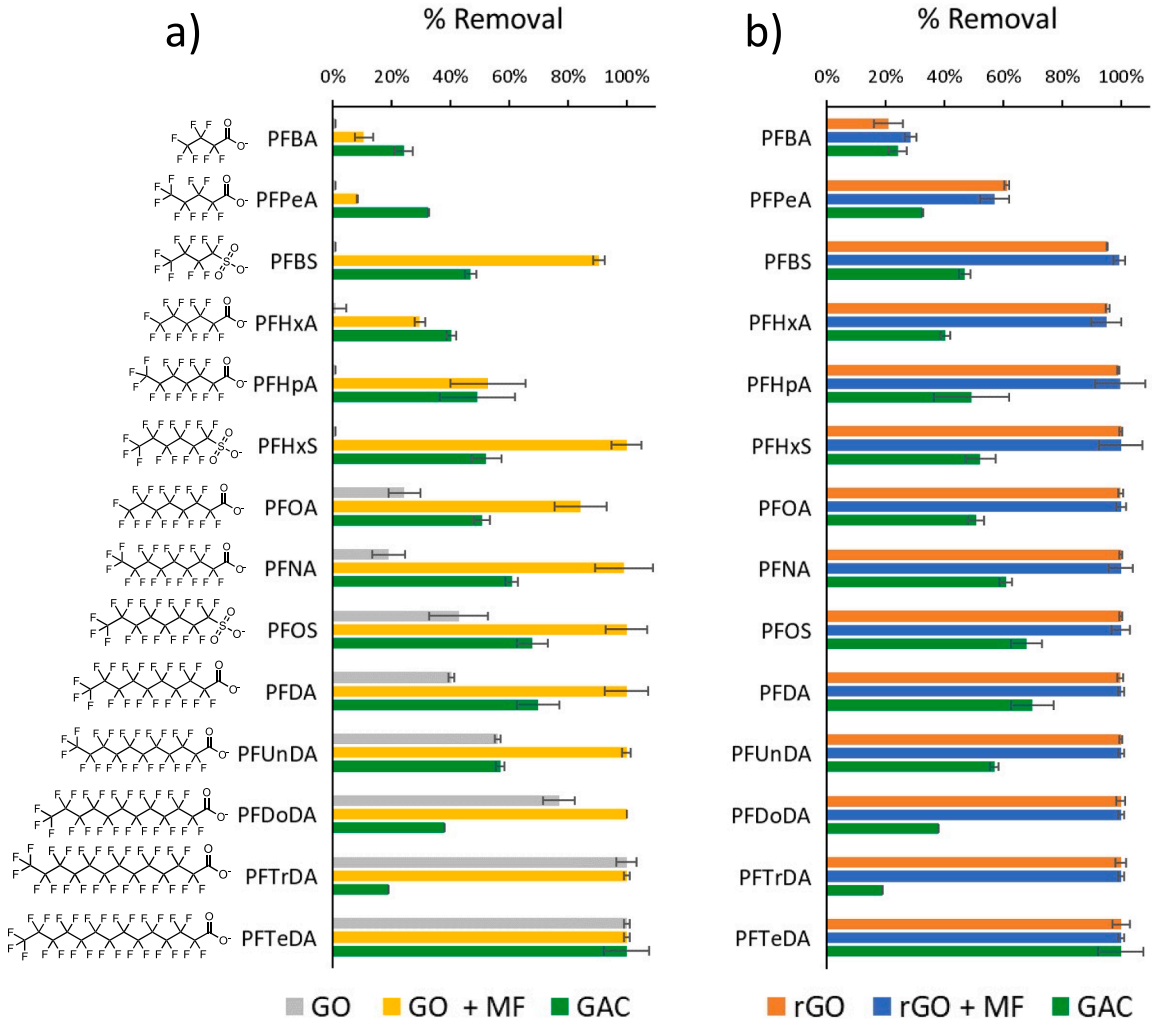

Fig. 7. Removal of PFASs from tap water. Removal by a) GO after 30 min of adsorption (GO, grey bars) and after adsorption and microfiltration (GO + MF, yellow bars), and b) by rGO after 30 min of adsorption (rGO, orange bars), after adsorption and microfiltration (rGO + MF, blue bars) and after adsorption on GAC (green bars). PFASs initial concentration 10 μg/L each.

respectively) as already observed by Wu et al. [30] showing that hydrophobic interactions, rather than electrostatic ones, dominated PFASs adsorption onto activated carbon.

The performance were compared to that of GAC [63,64], the standard adsorber used for PFASs removal in real potabilization plant. The MF + GO procedure removes about 72 μg/g of PFASs (total μg of PFASs per gram of sorbent), while the MF + rGO removed about 138 μg/g of PFASs (total μg of PFASs per gram of sorbent), while GAC after 30 min of contact time removed 44 μg/g of PFASs (total μg of PFASs per gram of sorbent; this last value increases up to 96.3 μg/g after 24 h), highlighting the higher suitability of rGO with respect to GO and the higher performance of both GO/rGO + MF procedure with respect to GAC for PFASs adsorption.

It is noteworthy that dedicated kinetic experiments highligthed the superior perfomance of rGO that, in just 10 min rather than 24 h required to GAC, expressesed most of its adsoprtion potential (Fig. S11 and Table S9, SI) with PFASs removals up to 3–5 times higher than GAC.

4. Conclusions

In conclusion, we presented a new methodology based on tandem adsorption on flocculated GO/rGO nanosheets and microfiltration, requiring only a few minutes to remove organic microcontaminants from drinking water. According to standard Italian regulation, potability was confirmed for GO/rGO + MF treated tap water and no evidence of graphene nanosheets release was found. The procedure exploited commercial GO and rGO nanosheets and commercially available hollow fiber microfiltration modules. The efficacy of the procedure on the removal of several classes of emerging contaminants (including OFLOX, a fluoroquinolone antibiotic) and PFASs was higher than that estimated for GAC adsorption under the same experimental conditions, in only few a minutes treatment.

The procedure has been here demonstrated for the removal of organic contaminants but it could be extended to the removal of metal cations, such as copper and lead, whose high performance adsorption of graphene has been widely demonstrated. It provides a complementary purification technology to the current standard adsorption on GAC for the removal of contaminants that are not efficiently removed by GAC. Moreover, synergy between graphene and hollow fiber MF modules could be exploited to combine depuration and sanitation in a single device. Indeed, MF modules, even Plasmart modules herein described, are already used as last step of purification in multitrain point-of-use devices for final disinfection of treated water. To this aim, automatization and prototyping of graphene addiction are ongoing in our lab.

Author contributions

M. Melucci wrote, revised, and edited the paper. A. Bianchi, S. Khaliha, M. Zambianchi, F. Tunioli performed the adsorption-filtration method optimization and application. A. Boschi, A. Liscio, D. Paci performed materials characterization. M. Navacchia, S. Valsecchi, S. Khaliha, M. Brunetti, M. Bergamini performed the analyses. A. Bianchi, S. Khaliha, A. Kovtun shared their first authorship. M. Melucci, V. Palermo, S. Polesello, L. Bocchi conceptualization, funding acquisition, resources, supervision, review, and editing. F. Tunioli, A. Kovtun, A. Bianchi drew the figures and revised the research paper. A. Bianchi, S. Khaliha, F. Tunioli, review and editing.

Declaration of Competing Interest

The authors declare that they have no known competing financial interests or personal relationships that could have appeared to influence the work reported in this paper.

Data Availability

All data generated or analysed during this study are included in this published article (and its supplementary information files).

Acknowledgements

This project has received funding from the European Union's Horizon 2020 research and innovation program under grant agreement No 881603, SH1 Graphil project, and from the FLAG-ERA III project GO-FOR-WATER, No 825207.

Appendix A. Supplementary material

Supplementary data to this article can be found online at https://doi.org/10.1016/j.seppur.2022.121826.

References

[1] B. Petrie, R. Barden, B. Kasprzyk-Hordern, A review on emerging contaminants in wastewaters and the environment: Current knowledge, understudied areas and recommendations for future monitoring, Water Res. 72 (2015) 3–27.
[2] R. Tröger, H. Ren, D. Yin, C. Postigo, P.D. Nguyen, C. Baduel, O. Golovko, F. Been, H. Joerss, M.R. Boleda, S. Polesello, M. Roncoroni, S. Taniyasu, F. Menger, L. Ahrens, F. Yin Lai, K. Wiberg, What's in the water? – Target and suspect screening of contaminants of emerging concern in raw water and drinking water from Europe and Asia, Water Res. 198 (2021) 117099.
[3] K.E. Murray, S.M. Thomas, A.A. Bodour, Prioritizing research for trace pollutants and emerging contaminants in the freshwater environment, Environ. Pollut. 158 (12) (2010) 3462–3471.
[4] R. Meffe, I. de Bustamante, Emerging organic contaminants in surface water and groundwater: A first overview of the situation in Italy, Sci. Total Environ. 481 (2014) 280–295.
[5] H.R. Mortaheb, M. Baghban Salehi, M. Rajabzadeh, Optimized hybrid PVDF/graphene membranes for enhancing performance of AGMD process in water desalination, J. Ind. Eng. Chem. 99 (2021) 407–421.
[6] Z. Xu, T. Wu, J. Shi, K. Teng, W. Wang, M. Ma, J. Li, X. Qian, C. Li, J. Fan, Photocatalytic antifouling PVDF ultrafiltration membranes based on synergy of graphene oxide and TiO2 for water treatment, J. Membr. Sci. 520 (2016) 281–293.
[7] N. Baig, Ihsanullah, M. Sajid, T.A. Saleh, Graphene-based adsorbents for the removal of toxic organic pollutants: A review, J. Environ. Manage. 244 (2019) 370–382.
[8] G. Ersan, O.G. Apul, F. Perreault, T. Karanfil, Adsorption of organic contaminants by graphene nanosheets: A review, Water Res. 126 (2017) 385–398.
[9] L. Jiang, Y. Liu, S. Liu, G. Zeng, X. Hu, X.i. Hu, Z. Guo, X. Tan, L. Wang, Z. Wu, Adsorption of Estrogen Contaminants by Graphene Nanomaterials under Natural Organic Matter Preloading: Comparison to Carbon Nanotube, Biochar, and Activated Carbon, Environ. Sci. Technol. 51 (11) (2017) 6352–6359.
[10] T.A. Tabish, F.A. Memon, D.E. Gomez, D.W. Horsell, S. Zhang, A facile synthesis of porous graphene for efficient water and wastewater treatment, Sci. Rep. 8 (1) (2018).
[11] N. Yousefi, X. Lu, M. Elimelech, N. Tufenkji, Environmental performance of graphene-based 3D macrostructures, Nat. Nanotechnol. 14 (2) (2019) 107–119.
[12] R.L. White, C.M. White, H. Turgut, A. Massoud, Z.R. Tian, Comparative studies on copper adsorption by graphene oxide and functionalized graphene oxide nanoparticles, J. Taiwan Inst. Chem. Eng. 85 (2018) 18–28.
[13] S.Z.N. Ahmad, W.N. Wan Salleh, A.F. Ismail, N. Yusof, M.Z. Mohd Yusop, F. Aziz, Adsorptive removal of heavy metal ions using graphene-based nanomaterials: Toxicity, roles of functional groups and mechanisms, Chemosphere 248 (2020) 126008.
[14] S. Mantovani, S. Khaliha, L. Favaretto, C. Bettini, A. Bianchi, A. Kovtun, M. Zambianchi, M. Gazzano, B. Casentini, V. Palermo, M. Melucci, Scalable synthesis and purification of functionalized graphene nanosheets for water remediation, Chem. Commun. 57 (31) (2021) 3765–3768.
[15] K. Balasubramani, N. Sivarajasekar, M.u. Naushad, Effective adsorption of antidiabetic pharmaceutical (metformin) from aqueous medium using graphene oxide nanoparticles: Equilibrium and statistical modelling, J. Mol. Liq. 301 (2020) 112426.
[16] I. Anastopoulos, I. Pashalidis, A.G. Orfanos, I.D. Manariotis, T. Tatarchuk, L. Sellaoui, A. Bonilla-Petriciolet, A. Mittal, A. Núñez-Delgado, Removal of caffeine, nicotine and amoxicillin from (waste)waters by various adsorbents. A review, J. Environ. Manage. 261 (2020) 110236.
[17] S. Khaliha, T.D. Marforio, A. Kovtun, S. Mantovani, A. Bianchi, M. Luisa Navacchia, M. Zambianchi, L. Bocchi, N. Boulanger, A. Iakunkov, M. Calvaresi, A.V. Talyzin, V. Palermo, M. Melucci, Defective graphene nanosheets for drinking water purification: Adsorption mechanism, performance, and recovery, FlatChem 29 (2021) 100283.
[18] W. Peng, H. Li, Y. Liu, S. Song, A review on heavy metal ions adsorption from water by graphene oxide and its composites, J. Mol. Liq. 230 (2017) 496–504.

[19] M.-P. Wei, H. Chai, Y.-L. Cao, D.-Z. Jia, Sulfonated graphene oxide as an adsorbent for removal of Pb²⁺ and methylene blue, in: J. Colloid Interface Sci., 524, 2018, pp. 297–305, https://doi.org/10.1016/j.jcis.2018.03.094.

[20] J. Geng, Y. Yin, Q. Liang, Z. Zhu, H. Luo, Polyethyleneimine cross-linked graphene oxide for removing hazardous hexavalent chromium: Adsorption performance and mechanism, Chem. Eng. J. 361 (2019) 1497–1510.

[21] D.R. Dreyer, S. Park, C.W. Bielawski, R.S. Ruoff, The chemistry of graphene oxide, Chem. Soc. Rev. 39 (1) (2010) 228–240.

[22] S. Guo, Y. Nishina, A. Bianco, C. Ménard-Moyon, A Flexible Method for Covalent Double Functionalization of Graphene Oxide, Angew. Chem. Int. Ed. 59 (4) (2020) 1542–1547.

[23] A. Kovtun, M. Zambianchi, C. Bettini, A. Liscio, M. Gazzano, F. Corticelli, E. Treossi, M.L. Navacchia, V. Palermo, M. Melucci, Graphene oxide–polysulfone filters for tap water purification, obtained by fast microwave oven treatment, Nanoscale 11 (2019) 22780–22787, https://doi.org/10.1039/C9NR06897J.

[24] F. Perreault, A. Fonseca de Faria, M. Elimelech, Environmental applications of graphene-based nanomaterials, ChSRv 44 (2015) 5861–5896, https://doi.org/10.1039/C5CS00021A.

[25] E.F. Aboelfetoh, A.E. Aboubaraka, E.-Z. Ebeid, Binary coagulation system (graphene oxide/chitosan) for polluted surface water treatment, J. Environ. Manage. 288 (2021) 112481.

[26] J. Glüge, M. Scheringer, I.T. Cousins, J.C. DeWitt, G. Goldenman, D. Herzke, R. Lohmann, C.A. Ng, X. Trier, Z. Wang, An overview of the uses of per- and polyfluoroalkyl substances (PFAS), Environ. Sci. Processes Impacts 22 (12) (2020) 2345–2373.

[27] D. Schrenk, M. Bignami, L. Bodin, J.K. Chipman, J. del Mazo, B. Grasl-Kraupp, C. Hogstrand, L. Hoogenboom, J.-C. Leblanc, C.S. Nebbia, E. Nielsen, E. Ntzani, A. Petersen, S. Sand, C. Vleminckx, H. Wallace, L. Barregård, S. Ceccatelli, J.-P. Cravedi, T.I. Halldorsson, L.S. Haug, N. Johansson, H.K. Knutsen, M. Rose, A.-C. Roudot, H. Van Loveren, G. Vollmer, K. Mackay, F. Riolo, T. Schwerdtle, Risk to human health related to the presence of perfluoroalkyl substances in food, EFSA J. 18 (9) (2020).

[28] R.O.f.E. HO (World Health Organization), Keeping our Water Clean: The Case of Water Contamination in the Veneto Region, Italy (Copenhagen), 2017.

[29] S. Valsecchi, M. Rusconi, M. Mazzoni, G. Viviano, R. Pagnotta, C. Zaghi, G. Serrini, S. Polesello, Occurrence and sources of perfluoroalkyl acids in Italian river basins, Chemosphere 129 (2015) 126–134, https://doi.org/10.1016/j.chemosphere.2014.07.044.

[30] C. Wu, M.J. Klemes, B. Trang, W.R. Dichtel, D.E. Helbling, Exploring the factors that influence the adsorption of anionic PFAS on conventional and emerging adsorbents in aquatic matrices, Water Res. 182 (2020) 115950.

[31] E. Gagliano, M. Sgroi, P.P. Falciglia, F.G.A. Vagliasindi, P. Roccaro, Removal of poly- and perfluoroalkyl substances (PFAS) from water by adsorption: Role of PFAS chain length, effect of organic matter and challenges in adsorbent regeneration, Water Res. 171 (2020) 115381.

[32] T. Jin, M. Peydayesh, R. Mezzenga, Membrane-based technologies for per- and poly-fluoroalkyl substances (PFASs) removal from water: Removal mechanisms, applications, challenges and perspectives, Environ. Int. 157 (2021) 106876.

[33] P.J.J. Alvarez, C.K. Chan, M. Elimelech, N.J. Halas, D. Villagrán, Emerging opportunities for nanotechnology to enhance water security, Nat. Nanotechnol. 13 (2018) 634–641, https://doi.org/10.1038/s41565-018-0203-2.

[34] P. Alipour Atmianlu, R. Badpa, V. Aghabalaei, M. Baghdadi, A review on the various beds used for immobilization of nanoparticles: Overcoming the barrier to nanoparticle applications in water and wastewater treatment, J. Environ Chem. Eng 9 (6) (2021) 106514.

[35] S. Lath, D.A. Navarro, D. Losic, A. Kumar, M.J. McLaughlin, Sorptive remediation of perfluorooctanoic acid (PFOA) using mixed mineral and graphene/carbon-based materials %, J. Environ. Chem. 15 (8) (2018) 472–480.

[36] J. Becanova, Z.S.S.L. Saleeba, A. Stone, A.R. Robuck, R.H. Hurt, R. Lohmann, A graphene-based hydrogel monolith with tailored surface chemistry for PFAS passive sampling, Environ. Sci.: Nano 8 (2021) 2894–2907, https://doi.org/10.1039/D1EN00517K.

[37] C. Zhao, J. Fan, D. Chen, Y. Xu, T. Wang, Microfluidics-generated graphene oxide microspheres and their application to removal of perfluorooctane sulfonate from polluted water, Nano Res. 9 (2016) 866–875, https://doi.org/10.1007/s12274-015-0968-7.

[38] N.B. Saleh, A. Khalid, Y. Tian, C. Ayres, I.V. Sabaraya, J. Pietari, D. Hanigan, I. Chowdhury, O.G. Apul, Removal of poly- and per-fluoroalkyl substances from aqueous systems by nano-enabled water treatment strategies, Environ. Sci. Water Res. Technol. 5 (2019) 198–208, https://doi.org/10.1039/C8EW00621K.

[39] D. Barker, A. Fors, E. Lindgren, A. Olesund, E. Schröder, Filter function of graphene oxide: Trapping perfluorinated molecules, J. Chem. Phys. 152 (2020) 024704, https://doi.org/10.1063/1.5132751.

[40] L. Liu, Y. Liu, B. Gao, R. Ji, C. Li, S. Wang, Removal of perfluorooctanoic acid (PFOA) and perfluorooctane sulfonate (PFOS) from water by carbonaceous nanomaterials: A review, Crit. Rev. Environ. Sci. Technol. 50 (2020) 2379–2414, https://doi.org/10.1080/10643389.2019.1700751.

[41] S. Deng, Q. Zhang, Y. Nie, H. Wei, B. Wang, J. Huang, G. Yu, B. Xing, Sorption mechanisms of perfluorinated compounds on carbon nanotubes, Environ. Pollut. 168 (2012) 138–144, https://doi.org/10.1016/j.envpol.2012.03.048.

[42] Q. Yu, S. Deng, G. Yu, Selective removal of perfluorooctane sulfonate from aqueous solution using chitosan-based molecularly imprinted polymer adsorbents, Water Res. 42 (2008) 3089–3097, https://doi.org/10.1016/j.watres.2008.02.024.

[43] C.T. Vu, T. Wu, Adsorption of short-chain perfluoroalkyl acids (PFAAs) from water/wastewater, Environ. Sci. Water Res. Technol. 6 (2020) 2958–2972, https://doi.org/10.1039/D0EW00468E.

[44] P. McCleaf, S. Englund, A. Östlund, K. Lindegren, K. Wiberg, L. Ahrens, Removal efficiency of multiple poly- and perfluoroalkyl substances (PFASs) in drinking water using granular activated carbon (GAC) and anion exchange (AE) column tests, Water Res. 120 (2017) 77–87, https://doi.org/10.1016/j.watres.2017.04.057.

[45] Z. Bano, S.A. Mazari, R.M.Y. Saeed, M.A. Majeed, M. Xia, A.Q. Memon, R. Abro, F. Wang, Water decontamination by 3D graphene based materials: A review, J. Water Process Eng. 36 (2020) 101404, https://doi.org/10.1016/j.jwpe.2020.101404.

[46] Z. Sun, S. Fang, Y.H. Hu, 3D Graphene Materials: From Understanding to Design and Synthesis Control, Chem. Rev. 120 (2020) 10336–10453, https://doi.org/10.1021/acs.chemrev.0c00083.

[47] Y. Shen, Q. Fang, B. Chen, Environmental Applications of Three-Dimensional Graphene-Based Macrostructures: Adsorption, Transformation, and Detection, Environ. Sci. Technol. 49 (2015) 67–84, https://doi.org/10.1021/es504421y.

[48] Y. Lin, Y. Tian, H. Sun, T. Hagio, Progress in modifications of 3D graphene-based adsorbents for environmental applications, Chemosphere 270 (2021) 129420.

[49] R. Mohd Firdaus, N. Berrada, A. Desforges, A.R. Mohamed, B. Vigolo, From 2D Graphene Nanosheets to 3D Graphene-based Macrostructures, Chem. –Asian J. 15 (19) (2020) 2902–2924.

[50] P. Srivastava, B. Singh, M. Angove, Competitive adsorption behavior of heavy metals on kaolinite, J. Colloid Interface Sci. 290 (1) (2005) 28–38.

[51] A. Kovtun, A. Bianchi, M. Zambianchi, C. Bettini, F. Corticelli, G. Ruani, L. Bocchi, F. Stante, M. Gazzano, T.D. Marforio, M. Calvaresi, M. Minelli, M.L. Navacchia, V. Palermo, M. Melucci, Core–shell graphene oxide–polymer hollow fibers as water filters with enhanced performance and selectivity, Faraday Discuss. 227 (2021) 274–290, https://doi.org/10.1039/C9FD00117D.

[52] P. Zhang, J.-L. Gong, G.-M. Zeng, C.-H. Deng, H.-C. Yang, H.-Y. Liu, S.-Y. Huan, Cross-linking to prepare composite graphene oxide-framework membranes with high-flux for dyes and heavy metal ions removal, Chem. Eng. J. 322 (2017) 657–666.

[53] W.C. Chong, Y.L. Choo, C.H. Koo, Y.L. Pang, S.O. Lai, Adsorptive membranes for heavy metal removal – A mini review, AIP Conf. Proc. 2157 (2019) 020005, https://doi.org/10.1063/1.5126540.

[54] J.F.a.K. Kenney, E.S., Percentile Ranks 3.6 in Mathematics of Statistics, Pt. 1, third ed., Van Nostrand, Princeton, NJ, 1962, pp. 38–39.

[55] C.-J. Shih, S. Lin, R. Sharma, M.S. Strano, D. Blankschtein, Understanding the pH-Dependent Behavior of Graphene Oxide Aqueous Solutions: A Comparative Experimental and Molecular Dynamics Simulation Study, Langmuir 28 (2012) 235–241, https://doi.org/10.1021/la203607w.

[56] I. Chowdhury, M.C. Duch, N.D. Mansukhani, M.C. Hersam, D. Bouchard, Colloidal Properties and Stability of Graphene Oxide Nanomaterials in the Aquatic Environment, Environ. Sci. Technol. 47 (2013) 6288–6296, https://doi.org/10.1021/es400483k.

[57] M. Zambianchi, M. Durso, A. Liscio, E. Treossi, C. Bettini, M.L. Capobianco, A. Aluigi, A. Kovtun, G. Ruani, F. Corticelli, M. Brucale, V. Palermo, M. L. Navacchia, M. Melucci, Graphene oxide doped polysulfone membrane adsorbers for the removal of organic contaminants from water, Chem. Eng. J. 326 (2017) 130–140.

[58] P. Bradder, S.K. Ling, S. Wang, S. Liu, Dye Adsorption on Layered Graphite Oxide, J. Chem. Eng. Data 56 (1) (2011) 138–141.

[59] Q. Kong, X. He, L.i. Shu, M.-S. Miao, Ofloxacin adsorption by activated carbon derived from luffa sponge: Kinetic, isotherm, and thermodynamic analyses, Process Saf. Environ. Prot. 112 (2017) 254–264.

[60] A. Molla, Y. Li, B. Mandal, S.G. Kang, S.H. Hur, J.S. Chung, Selective adsorption of organic dyes on graphene oxide: Theoretical and experimental analysis, ApSS 464 (2019) 170–177.

[61] Ş.I. Voicu, F. Aldea, A. Nechifor, Polysulfone-carbon Nanotubes Composite Membranes Synthesis and characterization, Rev. Chim. 61 (2010) 817–821.

[62] K.-U. Goss, The pKa Values of PFOA and Other Highly Fluorinated Carboxylic Acids, Environ. Sci. Technol. 42 (2008) 5032, https://doi.org/10.1021/es8011904.

[63] M. ELAbadsa, M. Varga, V.G. Mihucz, Removal of selected pharmaceuticals from aqueous matrices with activated carbon under flow conditions, Microchem. J. 150 (2019) 104079.

[64] R. Desmiarti, Y. Trianda, M. Martynis, A. Viqri, T. Yamada, F.S. Li, Phenol Adsorption in Water by Granular Activated Carbon from Coconut Shell, Int. J. Technol. 10 (2019) 1488–1497, https://doi.org/10.14716/ijtech.v10i8.3463.